

High-Energy Emission from the PSR B1259-63 System near Periastron

M. Tavani¹, J.E. Grove², W. Purcell³, W. Hermsen⁴, L. Kuiper⁴, P. Kaaret¹, E. Ford¹, R.B. Wilson⁵, M. Finger⁵, B.A. Harmon⁵, S.N. Zhang⁶, J. Mattox⁷, D. Thompson⁸, and J. Arons⁹

¹ Columbia Astrophysics Laboratory, Columbia University, New York, NY 10027, USA

² Code 7651, Naval Research Laboratory, Washington, DC 20375, USA

³ Department of Physics & Astronomy, Northwestern University, Evanston, IL 60208, USA

⁴ SRON-Utrecht, Sorbonnelaan 2, 3584 CA Utrecht, The Netherlands

⁵ NASA/MSFC, Huntsville, AL, 35812, USA

⁶ Universities Space Research Association, NASA/MSFC, Huntsville, AL, 35812, USA

⁷ Department of Astronomy, University of Maryland, College Park, MD 20742, USA

⁸ Code 662, NASA/Goddard Space Flight Center, Greenbelt, MD 20771, USA

⁹ Department of Astronomy, University of California at Berkeley, Berkeley, CA 94720, USA

Received ; Accepted

Abstract. We report the results of a CGRO multi-instrument 3-week observation of the binary system containing the 47 ms pulsar PSR B1259-63 orbiting around a Be star companion in a very eccentric orbit. The PSR B1259-63 binary is a unique system for the study of the interaction of a rapidly rotating pulsar with time-variable nebular surroundings. CGRO observed the PSR B1259-63 system in coincidence with its most recent periastron passage (January 3-23, 1994). *Unpulsed and non-thermal* hard X-ray emission was detected up to 200 keV, with a photon index 1.8 ± 0.2 and a flux of ~ 4 mCrab, corresponding to a luminosity of a few $\times 10^{34}$ erg/s at the distance of 2 kpc. The hard X-ray flux and spectrum detected by CGRO agrees with the X-ray emission measured by simultaneous ASCA observations. EGRET upper limits are significant, and exclude strong inverse Compton cooling in the PSR B1259-63 system. We interpret the observed non-thermal emission as synchrotron radiation of shocked electron/positron pairs of the relativistic pulsar wind interacting with the mass outflow from the Be star. Our results clearly indicate, for the first time in a binary pulsar, that high energy emission can be shock-powered rather than caused by accretion. Furthermore, the PSR B1259-63 system shows that shock acceleration can increase the original energy of pulsar wind particles by a factor $\gtrsim 10$, despite the high synchrotron and inverse Compton cooling rates near periastron. We also present results of an extensive search for pulsed gamma-ray emission from PSR B1259-63. The lack

of pulsations constrains models of gamma-ray emission from rapidly rotating pulsars.

Key words: Gamma-Ray Sources, X-ray: binaries, Pulsars: individual: PSR B1259-63, Shock Emission

1. Introduction

The PSR B1259-63 system contains a rapidly rotating radio pulsar with spin period $P = 47.76$ ms and spindown luminosity $L_p \simeq 9 \times 10^{35}$ erg s⁻¹ orbiting around a massive Be star companion in a highly elliptical orbit with orbital period ~ 3.4 yrs at an estimated distance $d \simeq 2$ kpc (Johnston et al. 1992, 1994, 1995; Manchester et al., 1995). Table 1 summarizes the main pulsar and orbital characteristics of the PSR B1259-63 system which is the only known binary where the interaction of a relativistic pulsar wind and a mass outflow from a Be star can be studied in detail. For its characteristics, the PSR B1259-63 system turns out to be an important astrophysical laboratory for the study of pulsars interacting with gaseous environments. Be stars are characterized by large mass outflows mainly concentrated in the equatorial plane of the massive star (e.g., Waters et al. 1988) and PSR B1259-63 is expected to interact with the Be star outflow especially near periastron. The nature of the pulsar/outflow interaction can be studied with the help of the high-energy emission (UV, X-rays, γ -rays) expected by the disruption of the Be star outflow and possible formation of shocks (Tavani, Arons & Kaspi, 1994; hereafter TAK94). For the

first time, the PSR B1259-63 system allows to study a strong pulsar/outflow interaction.

High-energy emission from the PSR B1259-63 system near periastron can be produced by several different mechanisms:

(1) *Accretion* onto the surface of the neutron star can occur with consequent bright X-ray/hard X-ray emission for large mass outflow rates and high density of material near periastron. An example of direct accretion is the 69 ms X-ray pulsar A0538-66 in the LMC which occasionally accretes with an X-ray luminosity near the Eddington limit $L_E \sim 10^{38} \text{ erg s}^{-1}$ (Skinner et al. 1982).

(2) *Propeller effect* emission, caused by gaseous material being temporarily trapped between the light cylinder and corotation radius of the pulsar (e.g., Illarionov & Sunyaev, 1975).

(3) *Pulsar/outflow interaction* caused by the shock of a relativistic pulsar wind in the mass outflow from the companion star can produce unpulsed high-energy emission (TAK94; Tavani & Arons, 1997, hereafter TA97). The pulsar radiation pressure (caused by a MHD wind of relativistic particles, electrons, positrons and possibly ions outflowing from the pulsar) can be large enough to withstand the compressing ram pressure of the Be star gaseous outflow near periastron. High-energy shock emission in pulsar binaries is currently poorly constrained, and before the discovery of PSR B1259-63, only the Crab nebula provided an astrophysical system unambiguously powered by a pulsar wind (e.g., Kennel & Coroniti, 1984). The PSR B1259-63 system is interesting in that it provides an environment where the pulsar-driven shock can be studied in hydrodynamical and radiative regimes totally different from the Crab nebula (TAK94).

(4) *Pulsed magnetospheric emission*. Several rapidly spinning radio pulsars have been detected at γ -ray energies (e.g., Thompson et al. 1994, hereafter Th94), and the PSR B1259-63 parameters are not dissimilar to those of other γ -ray pulsars. The pulsar age of PSR B1259-63 is relatively large ($\tau_p \equiv P/2\dot{P} \sim 3.3 \cdot 10^5$ yrs) and the inferred dipolar magnetic field is sufficiently small ($B \sim 3.3 \cdot 10^{11}$ G) to allow an interesting comparison of the detection (or lack thereof) of pulsed high-energy emission from PSR B1259-63 compared to other pulsars of similar age (Th94).

We have obtained data from all four CGRO instruments during a 3-week uninterrupted observation of PSR B1259-63 (January 3-23, 1994) which included the periastron passage of January 9, 1994. The faintness of the expected high-energy emission near periastron justified a long observation. The length of the observation was crucial in detecting an unambiguous signal from the source. The CGRO observation was carried out during an extended ‘eclipse’ of the pulsed radio signal from PSR B1259-63 (Johnston et al. 1996; hereafter J96). The absence of detectable pulsed radio emission near periastron clearly indicates the presence of circumbinary dispersing/absorbing

material in agreement with the expected radial structure of the Be star outflow.

Table 1*

| Astrometric, Spin, and Radio Parameters* | |
|--|---------------------------------------|
| Right Ascension, α (J2000) | 13h 02m 47.68(2)s |
| Declination, δ (J2000) | $-63^\circ 50' 08''.6(1)$ |
| Dispersion Measure, DM | 146.75(8) pc cm $^{-3}$ |
| Period, P | 47.762053919(4) ms |
| Spin-down Rate, \dot{P} | $2.2793(4) \times 10^{-15}$ |
| Period Epoch | MJD 48053.44 |
| Spin-down Luminosity, L_p | $8 \times 10^{35} \text{ erg s}^{-1}$ |
| Orbital Parameters | |
| Orbital Period, P_b | 1236.79(1) dy |
| Projected semi-major axis, $a_p \sin i$ | 1295.98(1) lt s |
| Longitude of periastron, ω | $138^\circ.6548(2)$ |
| Eccentricity, e | 0.869836(2) |
| Periastron Epoch, T_0 | MJD 48124.3581(2) |

* From Johnston et al. (1994).

2. Detection of unpulsed emission

2.1. OSSE analysis

OSSE is the only CGRO instrument which detected a positive flux from the field surrounding PSR B1259-63 (Grove et al. 1995). The OSSE tungsten slat collimator defines the $3.8^\circ \times 11.4^\circ$ field of view, which was chosen as a compromise allowing high sensitivity to both diffuse emission and point sources. Spectra are accumulated in a sequence of two-minute measurements of the source field alternated with two-minute, offset-pointed measurements of background. The pulsar is located in the galactic plane at 304.2° longitude, where galactic diffuse continuum emission is detectable by OSSE. To minimize the effect of the galactic emission, the observation of PSR B1259-63 was performed with the long axis of the collimator oriented perpendicular to the plane and centered on the pulsar. Background fields on either side, centered at 308.7° and 296.4° longitude, were selected to avoid nearby point sources such as the X-ray binaries GX301-2, Cen X-3, and 2S 1417-624. These objects, shown by the BATSE instrument on CGRO to be occasional emitters in the 20–50 keV band, are each suppressed by a factor of $> 10^2$ by the collimator and account for no detectable emission in the source field. Unavoidably, the source field contained the Be-star binary pulsar GX304-1; however, this X-ray pulsar has not been detected by BATSE in three years of daily observation. A total exposure time $T = 1.9 \times 10^5$ s of highest-quality data were collected in two OSSE detectors on the PSR B1259-63 source field, with approximately an equal time on the background fields.

The photon number spectrum from the PSR B1259-63 system is shown in Fig. 1. Emission at the level of ~ 4 mCrab is detected by OSSE from 50 keV to ~ 200

keV, with a total statistical significance of 4.8σ . The best-fit power law photon number spectrum for photon energies E in the 50–300 keV band is $dN_\gamma/dE = (2.8 \pm 0.7) \times 10^{-3} (E/100 \text{ keV})^{-\alpha} \text{ ph. cm}^{-2} \text{ s}^{-1} \text{ MeV}^{-1}$, with photon index $\alpha = 1.8 \pm 0.6$. The power-law fit is good ($\chi^2_{\text{dof}} = 0.90$ for 40 degrees of freedom). Also shown in Fig. 1 is the ASCA spectrum for the January 26, 1994 observation (Kaspi et al. 1995; hereafter KTN95). The emission in the OSSE band is consistent in intensity and spectral shape with a simple power-law extrapolation of the ASCA observation. The continuation of the power law spectrum to hard X-ray energies is very significant for the interpretation of the emission. At 2.0 kpc (Johnston et al. 1994), the inferred 50–200 keV luminosity of the PSR B1259-63 system is $L_X \simeq 3 \times 10^{34} \text{ erg s}^{-1}$, and the hardness of the OSSE spectrum suggests that the luminosity per energy decade peaks near or above 200 keV.

There is no evidence for variability in the OSSE data; however, because of the relatively low statistical significance of the detection, the constraints on variability are not stringent. The 95%-confidence upper limits on 50–200 keV variability on daily or weekly timescales are $\sim 190\%$ and $\sim 70\%$, respectively. Any flux decrease by $\sim 50\%$ during the 3-week observing period, as suggested by the ASCA data, is undetectable by OSSE.

For weak detections such as that from the PSR B1259-63 field, it is important to address possible systematic errors or alternate sources for the emission. A study of residuals in the 50–200 keV band from an aggregate of many OSSE pointings indicates that the systematic errors are smaller than the statistical errors and, therefore, that the $\sim 5\sigma$ excess reported here should be exceedingly rare. The background fields of view were chosen to exclude known point sources of hard X-rays in the region. From measurements near the galactic plane, and for a simple one-dimensional galactic plane model, we estimate that the large-scale (i.e. $\sim 10^\circ$) longitudinal gradient in the emission per degree in the 50–200 keV band is $\sim -3 \times 10^{-5} \text{ ph. cm}^{-2} \text{ s}^{-1} \text{ MeV}^{-1} \text{ deg}^{-2}$. Assuming that the diffuse emission is symmetric about the galactic center and convolving this emission through the instrument response, we estimate that the residual diffuse 50–200 keV flux for our viewing strategy of the PSR B1259-63 region is $\sim 2 \times 10^{-4} \text{ ph. cm}^{-2} \text{ s}^{-1} \text{ MeV}^{-1}$, a factor of ~ 10 less than the observed flux. We note, however, that the level of small-scale, local fluctuations in the diffuse emission is somewhat uncertain and not easily measured, given the presence of nearby point sources. Such fluctuations are the most likely alternative explanation for the observed flux.

2.2. BATSE analysis

BATSE data were analyzed near the time of periastron using the standard BATSE occultation technique. The resulting light curve spans the period of truncated Julian days (TJD) 9340–9380. No significant flux was detected,

with an upper limit of $\Phi_{\text{BATSE}} \lesssim 0.02 \text{ ph. cm}^{-2} \text{ s}^{-1}$ in the 20–120 keV energy band. This limit was obtained assuming a power law index of emission -2 in the deconvolution. This upper limit is ultimately a consequence of systematic effects which are observed as a scatter of the flux around a zero mean value. We notice that Φ_{BATSE} is about one order of magnitude larger than the detected flux by OSSE.

2.3. COMPTEL analysis

COMPTEL data for PSR B1259-63 from the VPs 314-316 were analyzed in four different energy channels at 1, 1-3, 3-10, 10-30 MeV. A spatial analysis was performed with the use of the maximum likelihood method to the three dimensional COMPTEL data space, which is defined by the coordinates of the scatter direction of the incoming photon in the upper-detector layer and by the scatter angle (Schoenfelder et al. 1993). The dominating background distribution in this data space has been determined applying a filter technique to the measured count distribution in the same data space. This approach produces a smooth background distribution in which source-like enhancements are suppressed. In order to verify that the background treatment does not suppress evidence for a genuine source signal at the position of PSR B1259-63, we applied three different approaches to the background generation. No evidence for a detection of the PSR B1259-63 system was found in the COMPTEL data.

2.4. EGRET analysis

We performed a spatial analysis of EGRET data using a maximum likelihood technique (Mattox et al. 1996). The observed intensity from the direction of PSR B1259-63 was compared with that one expected from the galactic and extragalactic diffuse γ -ray emission as modelled by Hunter et al. (1996). Upper limits (95% confidence) were derived from the likelihood analysis. We have also examined the EGRET data for γ -ray transient emission from the PSR B1259-63 system on time scales ranging from hours to several days. No significant transient emission was detected for photon energies $E_\gamma > 80 \text{ MeV}$. The most stringent constraints on high-energy radiation are provided by the spatial analysis for the whole data set (see Table 2).

3. Search for pulsations

Using the radio ephemeris of Table 1, we searched for pulsed emission at the rotation period of the pulsar calculated for the particular time of observation. The orbital motion introduces non-negligible Doppler shifts of the photon arrival times, and standard techniques were used to correct the observed photon arrival times to the pulsar barycenter. No pulsed emission was detected by any CGRO instrument. However, we caution that because of the long integration required in the γ -ray regime, small

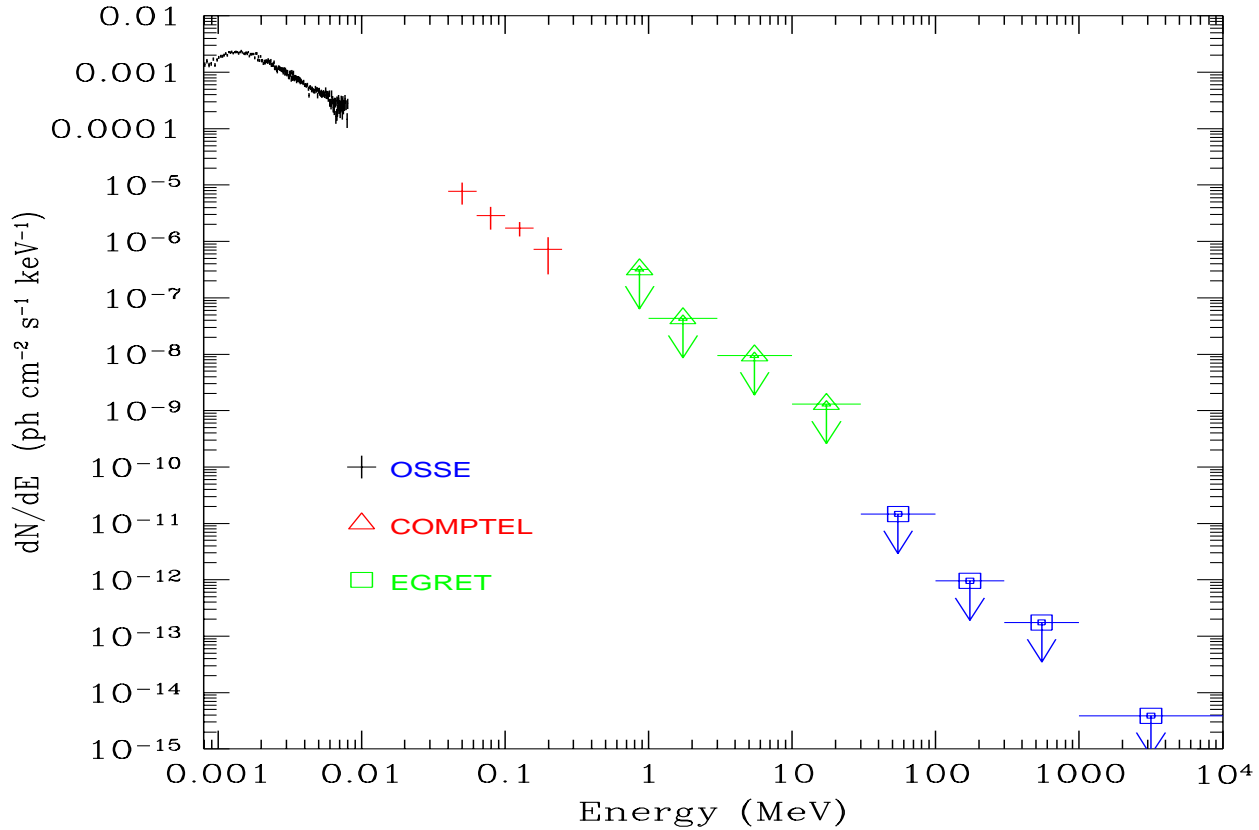


Fig. 1. GRO multi-instrument spectrum of PSR B1259-63 near periastron during the period January 3-23, 1994 (data from Grove et al. 1995). BATSE upper limits are not given, and they are a factor of ~ 10 larger than the OSSE data points. Also ASCA data (0.5-10 keV) obtained during the post-periastron January 26, 1994 observation are given for comparison (KTN95).

errors in the pulsar ephemeris could in principle smear coherent pulsations. Due to the relatively small flux detected from the PSR B1259-63 system, the best CGRO upper limits on pulsed emission were obtained in the OSSE energy range, corresponding to $\eta_{1259} \lesssim \eta_{Crab}$, where η is the efficiency of conversion of spindown energy into pulsed γ -ray emission.

The OSSE 95% confidence upper limits for pulse widths of 0.15 or 0.5 in the 50-180 keV band during the 21-day observation are $\Phi_{0.15} = 3 \cdot 10^{-4}$ and $\Phi_{0.5} = 6 \cdot 10^{-4}$ ph. cm $^{-2}$ s $^{-1}$ MeV $^{-1}$, respectively. The former limit corresponds to $\sim 3 \cdot 10^{-3}$ Crab pulsar flux units.

For pulse periods less than 1 s, BATSE data can be acquired in the ‘folded-on-board’ (FOB) mode. In this mode, data in the appropriately pointed Large Area Detectors undergo pre-telemetry folding at a specified period. FOB data, folded at the pulsar spin period, was obtained for the time intervals TJD 9341-9375 and TJD 9397-9433. The time coverage extends from approximately 20 days before periastron to 72 days later. In none of the folding time intervals we find a significant deviation from a flat light curve. We performed a Monte Carlo calculation to determine an upper limit of $\sim 1.5 \times 10^{-3}$ ph. cm $^{-2}$ s $^{-1}$

for Gaussian-shaped pulsed emission in the energy range 20-100 keV.

We carried out a timing analysis of COMPTEL data for the same energy channels used for the study of unpulsed emission. The applied event selections are based on experience gained in the analysis of the Crab and Vela pulsed signal. The data have been folded using the parameters of two different ephemerides (Johnston et al. 1994; J96). One for pre-periastron data, and one fitting all radio data up to May 1994. However, it should be realized that there is an uncertainty in the instantaneous phase during the periastron passage, with shifts possibly as large as several milliseconds. The derived phase histograms, for both ephemerides and energy intervals, do not show sufficient evidence for a pulsed signal.

Timing analysis of EGRET data in different energy intervals did not yield a positive detection of PSR B1259-63. Applying the technique of Thompson et al. (1994), upper limits are obtained in a search for a pulsed signal assuming a sinusoidal shape, as well as assuming a narrow pulse shape. The latter approach produces somewhat lower upper limits (see Table 2).

Table 2: EGRET 95% upper limits

| Energy Range (MeV) | $F^{(a)}$ | $F_E^{(b)}$ | $F_{np}^{(c)}$ | $F_{bp}^{(d)}$ |
|--------------------|-----------|-------------|----------------|----------------|
| 30-100 | 79. | 6.6 | 100. | 250. |
| 100-300 | 18. | 4.8 | 20. | 49. |
| 300-1000 | 9.4 | 7.8 | 9.6 | 23. |
| 1000-10000 | 4.5 | 18. | 7.3 | 21. |

(a) Photon flux upper limit (in units of $10^{-8} \text{ cm}^{-2} \text{ s}^{-1}$); (b) energy flux upper limit (in units of $10^{-11} \text{ erg cm}^{-2} \text{ s}^{-1}$); (c) flux upper limit of pulsed emission for a narrow pulse (in units of $10^{-8} \text{ cm}^{-2} \text{ s}^{-1}$); (d) flux upper limit of pulsed emission for a broad pulse (in units of $10^{-8} \text{ cm}^{-2} \text{ s}^{-1}$). The narrow and broad pulse light curves have been assumed to be Gaussian-shaped 10% wide in phase and a sinusoid, respectively.

By adopting an integrated energy upper limit ($E_\gamma > 100 \text{ MeV}$) $\Phi_{EGRET} \sim 10^{-11} \text{ erg cm}^{-2} \text{ s}^{-1}$ and a beaming factor $f_b = 1 \text{ sr}$, we obtain an upper limit to the efficiency η in the EGRET energy range $\eta'_{EGRET} \lesssim 0.005$. This upper limit is about a factor of 70 larger than in the case of the Crab in the same energy range. For comparison, we note that in the EGRET energy range the efficiencies for pulsed emission for the Vela pulsar and PSR 1706-44 are $\eta_{Vela} \sim 0.002$, and $\eta_{1706-44} \sim 0.007$, respectively. We conclude that the current EGRET upper limits on pulsed emission from PSR B1259-63 exclude a relatively large efficiency as for PSR 1706-44. Fig. 2 shows the pulsar parameter space with the inclusion of PSR B1259-63 and with the EGRET γ -ray pulsars clearly marked. We notice that PSR B1259-63 has parameters typically smaller by a factor of ~ 2 than those of PSR 1951+32 recently revealed by EGRET with an efficiency $\eta_{1951+32} \sim 0.0038$ (Ramanamurthy et al. 1995).

4. Comparison with radio and ASCA data near periastron

Extensive radio observations of PSR B1259-63 carried out in 1993 and 1994 (J96) showed a first sign of pulsar/outflow interaction in the PSR B1259-63 system in October 1993 (approximately at $\mathcal{T} - 94$, where $\mathcal{T} = \text{January 9.2, 1994}$, TJD 49361.7 is the periastron date). Substantial radio pulse depolarization was observed, with occasional eclipsing behavior at 1.5 GHz at the end of November 1993. The pulsar was not detected in 1.5 GHz data on Dec. 20, 1993 ($\mathcal{T} - 20$) and reappeared on Feb. 4, 1994 ($\mathcal{T} + 24$). During the 44-day eclipse PSR B1259-63 was not detected in extensive observations at 1.5 and 8.4 GHz (J96). The dispersion measure showed substantial increase in the pre-eclipse data, reaching a value of $\Delta DM \sim 11 \text{ cm}^{-3} \text{ pc}$ above normal, corresponding to an average free electron density of $N_e \sim 3.3 \cdot 10^{19} \text{ cm}^{-2}$. By mid-April 1994, both the linear polarization and the rotation measure were back to pre-eclipse values. Extensive ASCA observations of the PSR B1259-63 system near and after periastron (see Fig. 1; KTN95, Hirayama et al. 1996, TA97) show a non-thermal X-ray

spectrum with luminosity $L_X \sim 10^{34} \text{ erg s}^{-1}$ and photon index $1.9 - 1.6$. The deduced column density to photoabsorbing atoms is particularly low $N_H \simeq 5 \cdot 10^{21} \text{ cm}^{-2}$, and consistent with negligible intrinsic absorption. Furthermore, N_H was observed to be constant throughout the whole set of ASCA observations covering the periastron passage of PSR B1259-63. A crucial ASCA observation of PSR B1259-63 carried out on Feb. 28, 1994 (when pulsed radio emission from PSR B1259-63 was again visible, J96) gave X-ray intensity, spectrum and column density similar to those previously observed near periastron (Hirayama et al. 1996). We conclude that both the radio and the X-ray data on PSR B1259-63 are consistent with a relatively ‘dilute’ nebular environment surrounding PSR B1259-63 near periastron and in sharp contrast with environments surrounding accreting systems.

5. Theoretical discussion

Hard X-ray emission with a photon index $\alpha \sim 1.8 - 2$ is a manifestation of energetic particle acceleration. Accreting neutron stars tend to be episodic emitters in the hard X-ray band typically with soft thermal or steep power law (photon index > 3) spectra (e.g. Barret & Vedrenne 1994). In the case of emission from the PSR B1259-63 system, one can argue against accretion or propeller mechanisms because of: (A) lack of X-ray/ γ -ray pulsations, (B) absence of significant X-ray fluctuations within timescales of order of days or less (KTN95), (C) relatively low X-ray luminosity and negligible absorption column density (TA97), (D) hardness of the power-law X-ray spectrum up to $\sim 200 \text{ keV}$. For the parameters of the PSR B1259-63 system, it can be shown that accretion or propeller regimes near periastron are unlikely to occur except for unusually large values of the the mass loss rate from the Be star companion (TA97).

Hard X-rays provide crucial information on the shock emission due to the interaction of the relativistic particle wind of PSR B1259-63 with the nebular gas of the Be star mass outflow. As in the case of the Crab nebula (Kennel & Coroniti 1984, Gallant & Arons 1994), shock acceleration and synchrotron radiation capable of producing unpulsed hard X-ray emission occurs at a shock radius within the PSR B1259-63 binary where pressure balance is established (TAK94) between the pulsar relativistic wind (electrons/positrons, possibly ions) and the ram pressure of the Be star outflow. The radiative environment near the shock radius within the PSR B1259-63 system is quite different from that of the Crab nebula, and the large synchrotron and inverse Compton cooling rates ($\sim 10^{-2} - 10^{-3} \text{ s}^{-1}$) at the PSR B1259-63 periastron make the detection of high-energy emission a unique diagnostic of shock acceleration subject to strong radiative cooling. By comparing the CGRO and ASCA results a unified picture for the emission and spectrum emerges. Spectral calculations for models with a weak ram pressure

of the Be star outflow show that the dominating inverse Compton spectrum is typically much too flat to agree with the OSSE data (TA97).

The spectral shape and intensity of the power-law emission from the PSR B1259-63 system are consistent with synchrotron radiation of shock-accelerated electron-positron pairs for an intermediate value of the ram pressure of the Be star outflow and a shock distance relatively close to the pulsar rather than to the Be star. The inferred characteristics of the electron/positron pairs in the pulsar wind are a Lorentz factor of $\gamma_1 \sim 10^6$ and a ratio of electromagnetic energy density to particle kinetic energy density in the wind of $\sigma \sim 10^{-1} - 10^{-2}$ (TA97). The observed efficiency of conversion of the PSR B1259-63 pulsar wind kinetic and electromagnetic energy into radiation in the 50-200 keV band is $\sim 3\%$, i.e., a value comparable to the efficiency of the Crab nebula. The absence of a spectral break from the soft X-ray band above the photon energy $\epsilon_{min} \sim 1$ keV through the lower limit on the high-energy cutoff, $\epsilon_{max} \gtrsim 200$ keV from the OSSE detection, and the COMPTEL and EGRET upper limits strongly constrains the acceleration mechanism. The collisionless pulsar wind shock must produce a power-law particle distribution function of index δ between a minimum e^\pm -pair energy $E_1 = \gamma_1 m_e c^2$ and an upper energy cutoff $E_c = \gamma_c m_e c^2$, with m_e the electron-positron mass and c the speed of light. For a synchrotron model of shock emission, we obtain the interesting constraint (TA97)

$$\frac{\gamma_c}{\gamma_1} \gtrsim \left(\frac{\epsilon_{max}}{\epsilon_{min}} \right)^{1/2} \sim 10, \quad (1)$$

where $\epsilon_{max} \simeq 200$ keV. Furthermore, we obtain $\delta = 2\alpha - 1 \sim 2 - 3$. A spectral cutoff is likely to occur near 1-10 MeV, in agreement with the calculated spectra for pulsar wind termination shocks subject to strong radiative cooling (TA97). The CGRO observation of the PSR B1259-63 system therefore demonstrates, for the first time in a galactic source, the ability of shock acceleration to efficiently energize a relativistic plasma subject to radiative cooling of typical timescales $\tau_c \sim 10^2 - 10^3$ s. The important derived constraints on the radiation efficiency ($\sim 3\%$), acceleration timescale ($\lesssim \tau_c$), index of the post-shock particle distribution ($\delta \sim 2 - 3$) are of crucial interest for any theory of relativistic shock acceleration.

Acknowledgements. We thank S. Johnston and R.N. Manchester for useful exchange of information, and F. Nagase and V. Kaspi for discussions and collaborative effort on the ASCA data. Research supported by NASA grant NAG5-2234.

6. References

Barret, D. & Vedrenne, G. 1994, ApJS, 92, 505 .
 Gallant, Y.A., & Arons, J. 1994, ApJ, 435, 230.
 Grove, J.E., et al., 1995, ApJ, 447, L112.
 Hirayama, M., et al. , 1996, to be submitted to PASP.

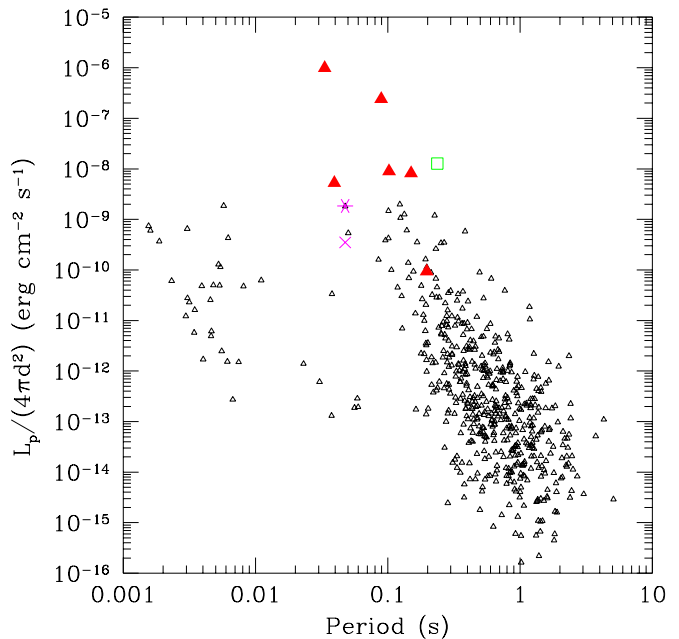


Fig. 2. Distribution of pulsar spindown energy flux vs. pulsar spin period for 706 pulsars. L_p and d are the pulsar spindown luminosities and distances (Taylor et al. 1993). Large triangles indicate detected gamma-ray pulsars (Thompson et al. 1994). Geminga parameters (for an assumed distance of 150 pc) are marked by an open square. The star and the tilted cross mark the parameters of PSR B1259-63 for $d = 2$ kpc (J96) and $d = 4.6$ kpc (Taylor et al. , 1993), respectively.

Hunter, S. et al. , 1996, ApJ, in press.
 Illarionov A.F. & Sunyaev, R.A., 1975, A&A, 39, 185.
 Johnson, W.N., et al. 1993, ApJS, 86, 693.
 Johnston, S., et al., 1992 ApJ, 387, L37.
 Johnston, S., et al. , 1994, MNRAS, 268, 430.
 Johnston, S., et al. , 1996, MNRAS, 279, 1026 (J96).
 Kaspi, V., Tavani, M., Nagase, F., Hoshino, M., Aoki, T., Hirayama, M., Kawai, N. & Arons, J., 1995, ApJ, 453, 424 (KTN95).
 Kennel, C.F. & Coroniti, F.V. 1984, ApJ, 283, 694.
 Manchester, R.N. et al. , 1995, ApJ, 445, L137.
 Mattox, J., et al. , 1996, ApJ, in press.
 Purcell, W.R., et al., 1994, in AIP Conf. Proc. 304, p. 403.
 Skinner, G.K., et al. , 1982, Nature, 297, 568.
 Ramanamurthy et al. , 1995, ApJ, 447, L109.
 Schoenfelder V. et al. , 1993, ApJS, 86, 657.
 Tavani, M., Arons, J., Kaspi, V. 1994, ApJ, 433, L37.
 Tavani, M. & Arons, J., 1997, ApJ, in press; astro-ph/9610212 (TA97).
 Taylor, J., Manchester, R., Lyne, A., 1993, ApJS, 88, 529.
 Thompson, D., et al., 1994, ApJ, 436, 229 (Th94).
 Waters, L.B.F.M., et al. 1988, A&A, 198, 200.
 White, N.E., Nagase, F. & Parmar, A.N. 1995, in *X-Ray Binaries* (Cambridge Univ. Press), p. 1.

This article was processed by the author using Springer-Verlag
L^AT_EX A&A style file *L-AA* version 3.